Arabidopsis cyclophilins direct plasmodesmata-targeting of mobile mRNA via organelle hitchhiking

Kai-Ren Luo[1], Nien-Chen Huang[1], Yu-Hsin Chang[2], and Tien-Shin Yu[1,*]

Supplementary information

Supplementary figure legends

Supplementary Figure 1. **PD-targeting of *FT* mRNA is independent of Golgi transport.** (a) Illustration of the MS2-based mRNA live-cell imaging system (left panel). The free form of nucleus-localized $MS2_{FD}$-GFP is restricted in the nucleus but translocates to cytosol upon interacting with mRNA containing the MS2-interaction stem loop (FT_{SL24}). The system distinguishes punctate distribution of mobile *FT* mRNA at the cell periphery (middle panel), compared to homogenous cytoplasmic localization of non-mobile *RFP* mRNA (right panel). Scale bar = 10 μm. (b) Independent transport of *FT* mRNA and Golgi (MAN49-mCherry) in transvacuolar strands between the nucleus (N) and cell cortex (arrowhead). Exemplified $MS2_{FD}$-GFP-labeled *FT* mRNA on transvacuolar strands is indicated by an arrow. Scale bar = 10 μm. (c) Brefeldin A (BFA) treatment relocates the Golgi marker MAN49-mCherry to ER. Scale bar = 5 μm. (d) BFA treatment had no effect on PD-targeting of *FT* mRNA. Note that *FT* mRNA puncta are observed in cells under BFA treatment and DMSO control. Scale bar = 10 μm.

Supplementary Figure 2. *AGL24* mRNA attaches to MVB for PD-targeting. Concanamycin A (CMA) treatment induced aggregation and cytosolic retention of RAB5-positive compartments. *AGL24* mobile mRNA remained attached on the organelles (indicated by white arrows) and failed to target to PD. Scale bar = 10 μm.

Supplementary Figure 3. Co-transport of *FT* mRNA and MVBs. Co-expression of $MS2_{FD}$-GFP-labeled *FT* mRNA (green) and mCherry-RAB5-positive MVBs (magenta) in *N. benthamiana* leaves by agro-infiltration. Images were captured with time points for each row indicated in left column. In middle column, yellow arrows indicated the track for fluorescence

intensity analysis. Right column illustrates the intensity profile, which suggested that *FT* mRNA was mostly decorated on the surface of RAB5-containing compartments. Scale bar = 2 μm.

Supplementary Figure 4. Cell-to-cell movement of putative endosome-localized RNA-binding proteins in Arabidopsis. Transient co-expression of DsRed with EGFP-labeled (a) AT1G18080 or (b) AT5G47210 by particle bombardment to Arabidopsis leaf epidermal cells. Scale bar = 20 μm.

Supplementary Figure 5. *in vivo* expression pattern and level of Arabidopsis cytoplasmic ROCs. (a) GUS expression driven by ROC promoters in Arabidopsis seedlings. Scale bar = 1 mm. (b) GUS expression driven by ROC promoters in Arabidopsis root. Scale bar = 0.1 mm. (c) *In planta* level of *ROC1, 2, 3, 5,* and *6* mRNAs relative to *UBIQUTIN CONJUGATION ENZYME* mRNA level, set to 1. Data are mean ± SD.

Supplementary Figure 6. Cytoplasmic ROCs (ROC1, 2, 3, 5, and 6), but not ER-localized ROC7, are mobile proteins. Expression pattern in root cells of GFP, GFPER (GFP-KDEL), and GFP-fused ROC proteins driven by *SUC2* promoter. Scale bar = 50 μm.

Supplementary Figure 7. Characterization of Arabidopsis ROCs mutant lines. (a) DNA sequencing analysis of *roc1* heterozygotic mutant generated by the CRISPR-Cas9 system. A 2-bp deletion, which results in a frameshift-sequence (indicated by an arrow), was detected in the *roc1* mutant. (b) Insertion site of T-DNA in *roc* mutant alleles. Numbers correspond to nucleotide position of T-DNA insertion relative to ATG (set to 1). Black blocks, exons; open blocks, untranslated regions. (c) RT-PCR analysis of ROC genes expression in corresponding T-DNA insertion lines. In the *roc2* mutant, the amplified DNA fragment of ROC2 gene is indicated by arrow. Actin was used as a loading control.

Supplementary video legends

Supplementary Video 1. Co-localization of $MS2_{FD}$-GFP-labeled *FT* mRNA and mCherry-labeled actin microfilament (Lifeact) during transport along transvacuolar strands connecting the nucleus (N) and cell cortex. Time is in minutes: seconds.

Supplementary Video 2. Transport-arrested $MS2_{FD}$-GFP-labeled *FT* mRNA and MAN49-mCherry-labeled Golgi in cytoplasmic space from cells with latrunculin B treatment. Time is in minutes: seconds.

Supplementary Video 3. Depletion of PD-targeting of $MS2_{FD}$-GFP-labeled *FT* mRNA in cells with oryzalin treatment. Time is in seconds.

Supplementary Video 4. Co-localization of $MS2_{FD}$-GFP-labeled *FT* mRNA and enlarged mCherry-labeled RAB5 vesicles in cells with concanamycin A treatment. Time is in minutes: seconds.

Supplementary table

Supplementary table 1. Putative endosome-localized RNA-binding proteins

Gene ID	Description
AT1G18080	Transducin/WD40 repeat-like superfamily protein
AT4G34870	Rotamase cyclophilin 5
AT5G47210	Hyaluronan / mRNA binding family

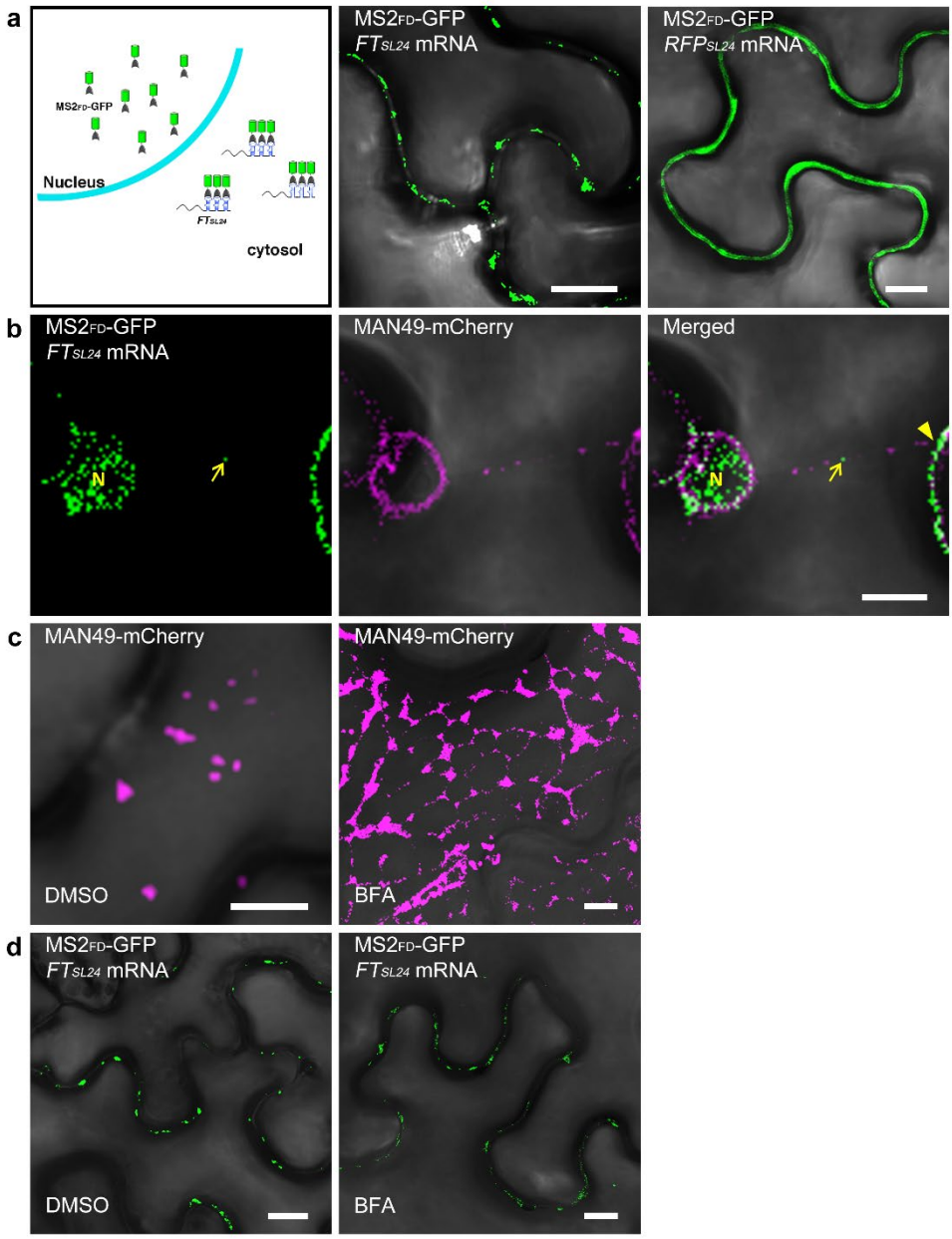

Luo et al., Supplementary Fig. 1

Supplementary Figure 1. **PD-targeting of *FT* mRNA is independent of Golgi transport.** (a) Illustration of the MS2-based mRNA live-cell imaging system (left panel). The free form of nucleus-localized MS2$_{FD}$-GFP is restricted in the nucleus but translocates to cytosol upon interacting with mRNA containing the MS2-interaction stem loop (*FT*$_{SL24}$). The system distinguishes punctate distribution of mobile *FT* mRNA at the cell periphery (middle panel), compared to homogenous cytoplasmic localization of non-mobile *RFP* mRNA (right panel). Scale bar = 10 µm. (b) Independent transport of *FT* mRNA and Golgi (MAN49-mCherry) in

transvacuolar strands between the nucleus (N) and cell cortex (arrowhead). Exemplified $MS2_{FD}$-GFP-labeled *FT* mRNA on transvacuolar strands is indicated by an arrow. Scale bar = 10 μm. (c) Brefeldin A (BFA) treatment relocates the Golgi marker MAN49-mCherry to ER. Scale bar = 5 μm. (d) BFA treatment had no effect on PD-targeting of *FT* mRNA. Note that *FT* mRNA puncta are observed in cells under BFA treatment and DMSO control. Scale bar = 10 μm.

Luo et al., Supplementary Fig. S2

Supplementary Figure 2. *AGL24* mRNA attaches to MVB for PD-targeting. Concanamycin A (CMA) treatment induced aggregation and cytosolic retention of RAB5-positive compartments. *AGL24* mobile mRNA remained attached on the organelles (indicated by white arrows) and failed to target to PD. Scale bar = 10 μm.

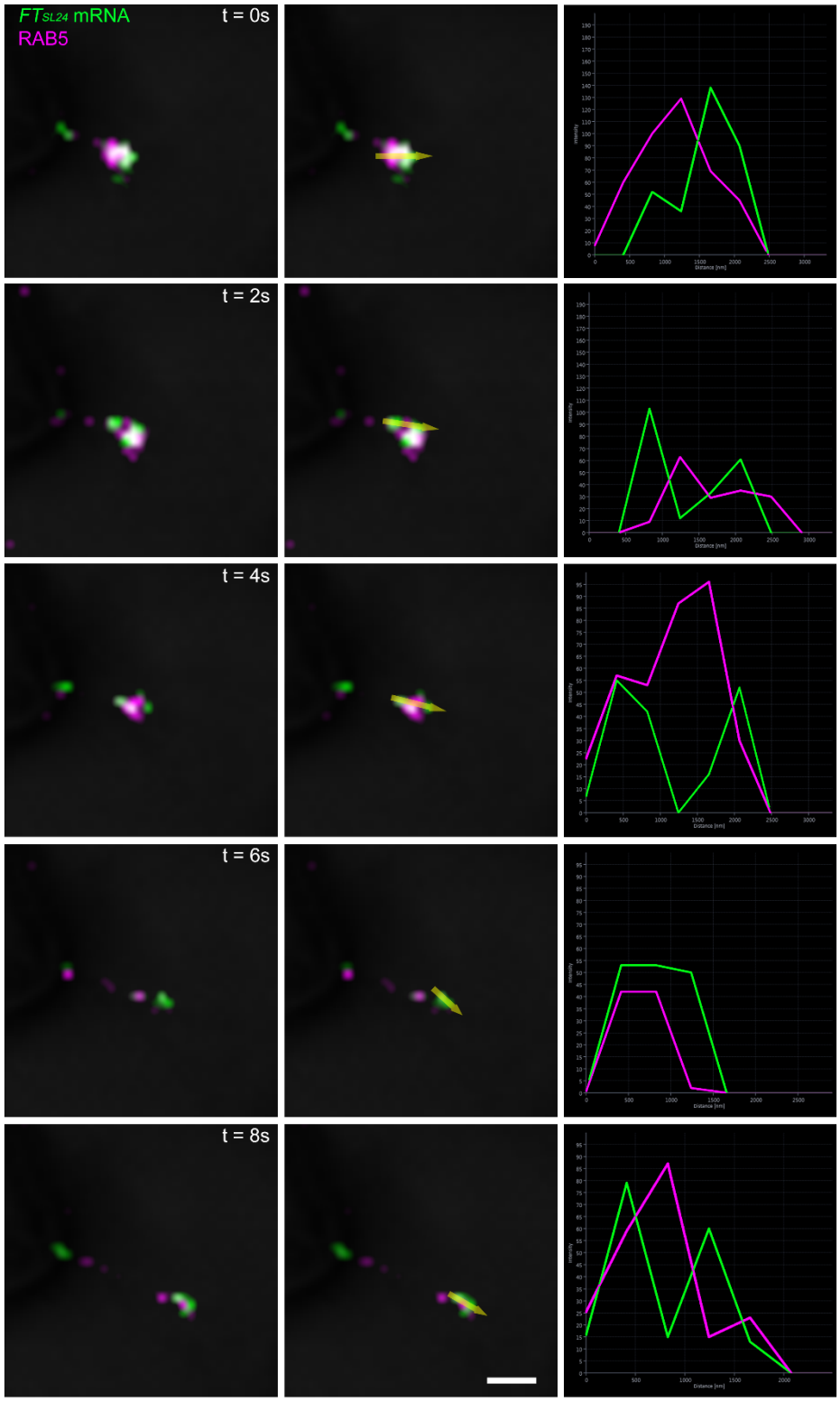

Luo et al., Supplementary Fig. 3

Supplementary Figure 3. Co-transport of *FT* mRNA and MVBs. Co-expression of MS2$_{FD}$-GFP-labeled *FT* mRNA (green) and mCherry-RAB5-positive MVBs (magenta) in *N.*

benthamiana leaves by agro-infiltration. Images were captured with time points for each row indicated in left column. In middle column, yellow arrows indicated the track for fluorescence intensity analysis. Right column illustrates the intensity profile, which suggested that *FT* mRNA was mostly decorated on the surface of RAB5-containing compartments. Scale bar = 2 μm.

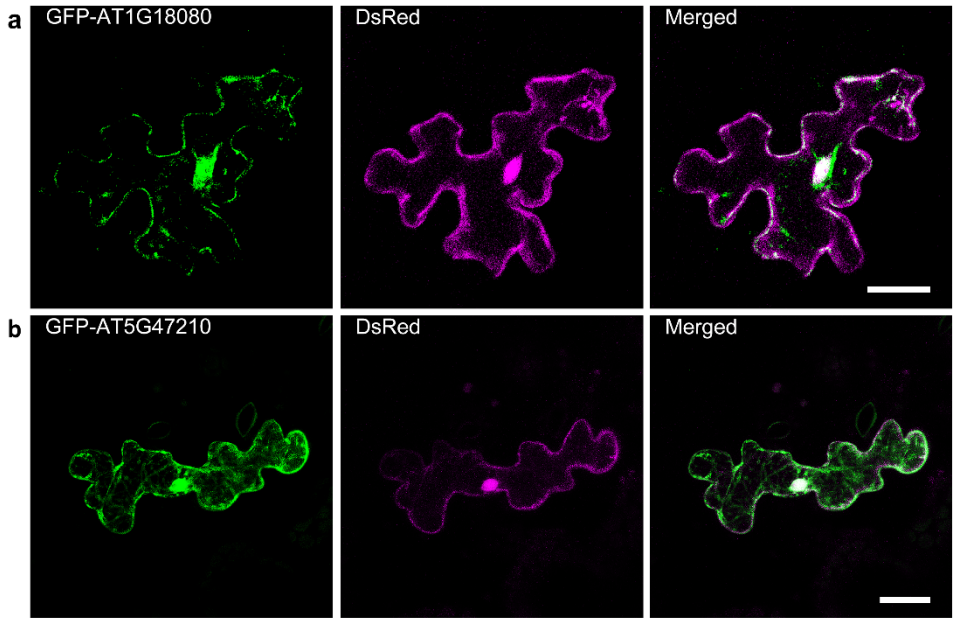

Luo et al., Supplementary Fig. 4

Supplementary Figure 4. Cell-to-cell movement of putative endosome-localized RNA-binding proteins in Arabidopsis. Transient co-expression of DsRed with EGFP-labeled (a) AT1G18080 or (b) AT5G47210 by particle bombardment to Arabidopsis leaf epidermal cells. Scale bar = 20 μm.

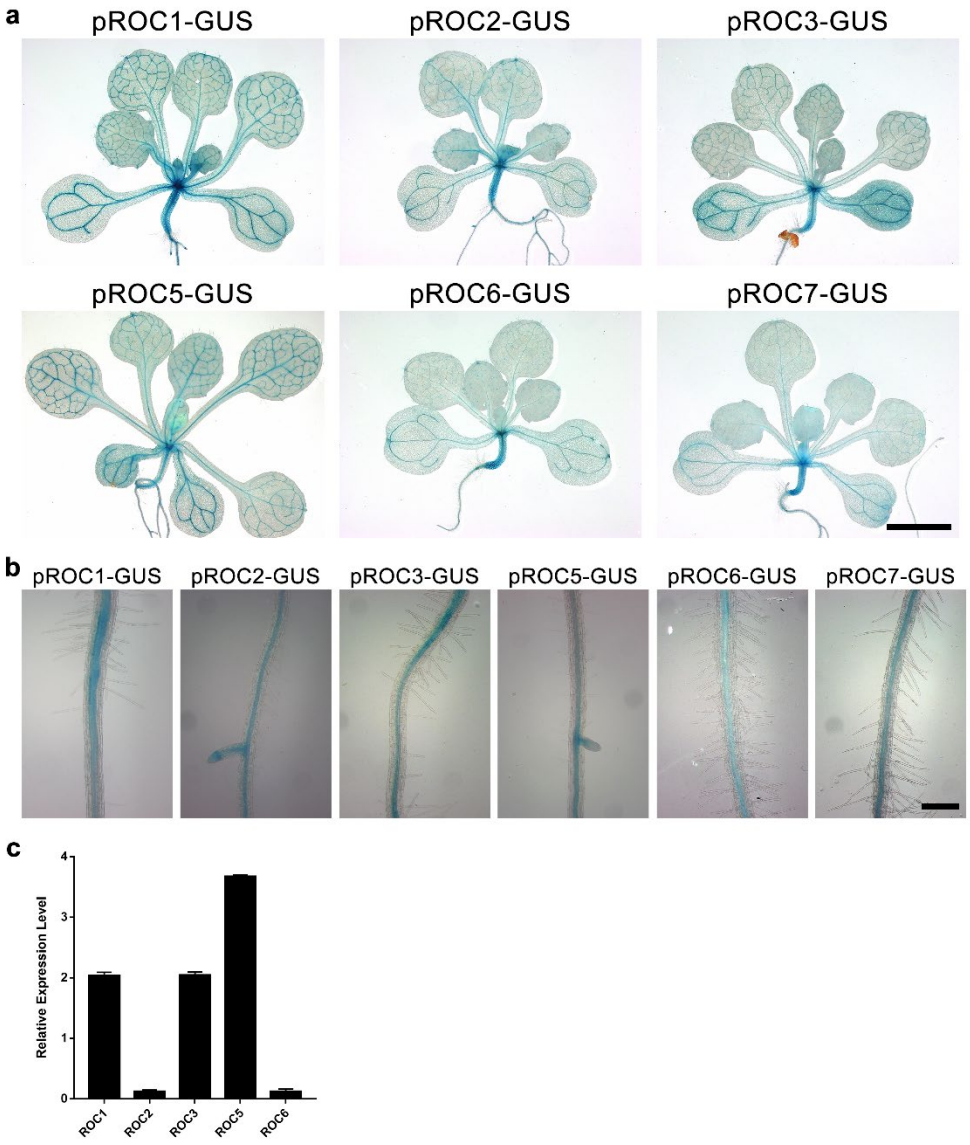

Luo et al., Supplementary Fig. 5

Supplementary Figure 5. *in vivo* expression pattern and level of Arabidopsis cytoplasmic ROCs. (a) GUS expression driven by ROC promoters in Arabidopsis seedlings. Scale bar = 1 mm. (b) GUS expression driven by ROC promoters in Arabidopsis root. Scale bar = 0.1 mm. (c) *In planta* level of *ROC1, 2, 3, 5,* and *6* mRNAs relative to *UBIQUTIN CONJUGATION ENZYME* mRNA level, set to 1. Data are mean ± SD.

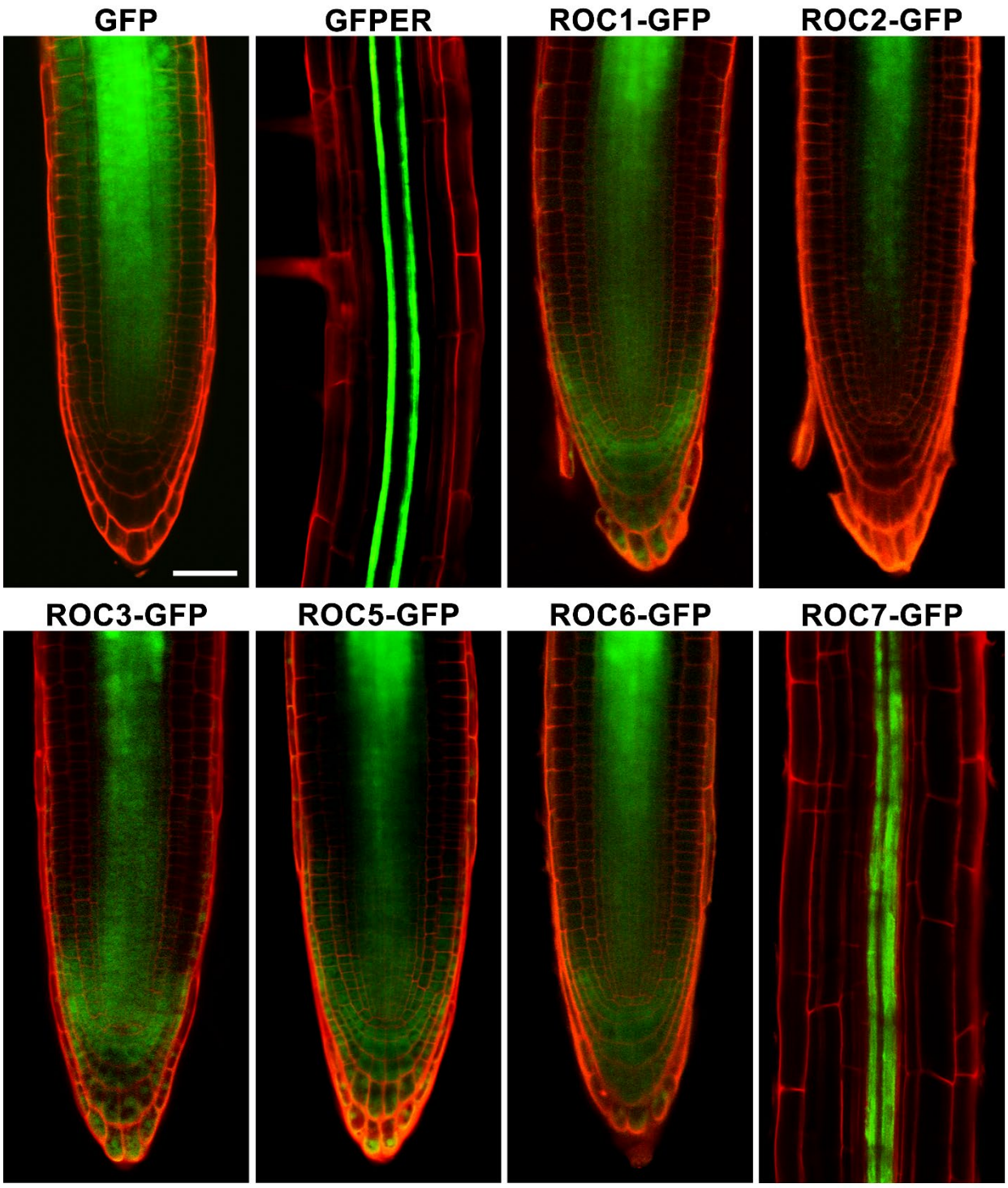

Luo et al., Supplementary Fig. 6

Supplementary Figure 6. Cytoplasmic ROCs (ROC1, 2, 3, 5, and 6), but not ER-localized ROC7, are mobile proteins. Expression pattern in root cells of GFP, GFPER (GFP-KDEL), and GFP-fused ROC proteins driven by *SUC2* promoter. Scale bar = 50 μm.

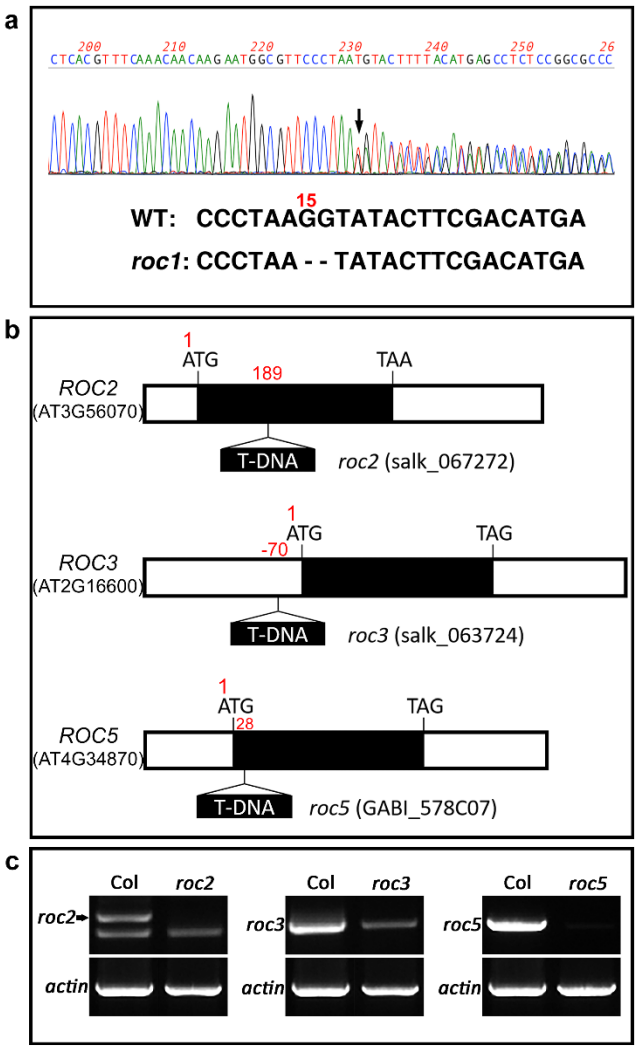

Luo et al., Supplementary Fig. 7

Supplementary Figure 7. Characterization of Arabidopsis ROCs mutant lines. (a) DNA sequencing analysis of *roc1* heterozygotic mutant generated by the CRISPR-Cas9 system. A 2-bp deletion, which results in a frameshift-sequence (indicated by an arrow), was detected in the *roc1* mutant. (b) Insertion site of T-DNA in *roc* mutant alleles. Numbers correspond to nucleotide position of T-DNA insertion relative to ATG (set to 1). Black blocks, exons; open blocks, untranslated regions. (c) RT-PCR analysis of ROC genes expression in corresponding T-DNA insertion lines. In the *roc2* mutant, the amplified DNA fragment of ROC2 gene is indicated by arrow. Actin was used as a loading control.